Interfacial-Energy-Controlled Deposition Technique of Microstructures Using Blade-Coating

Hidekazu Arase* and Tohru Nakagawa

Advanced Technology Research Laboratories, Panasonic Corporation. 3-4 Hikaridai, Seika-cho, Soraku-gun, Kyoto 619-0237, Japan

Received: July 23, 2009; Revised Manuscript Received: October 7, 2009

A novel blade-coating technique for the fluidic self-assembly of microstructures on large-scale substrates is presented. In our blade-coating technique, water and microstructures dispersion, which includes chemically modified microstructures and water-insoluble solvent, are continuously blade-coated on a substrate on which surface hydrophilic areas are surrounded by a hydrophobic self-assembled monolayer. In the process studied, first, water is selectively placed on the hydrophilic areas; second, the water-insoluble solvent covers the water to create a solvent/water interface; third, fluidic self-assembly of microstructures onto the water takes place by a capillary force between the water and the microstructures; and finally, the microstructures are deposited onto the hydrophilic areas after the evaporation of the water and the solvent. SiO_2 plates sized $10 \times 50 \times 0.3$ μm^3 were used to verify the feasibility of our technique. About 40 000 SiO_2 plates were selectively deposited on the hydrophilic areas on a substrate with an area of 20 cm^2 with a deposition probability of 0.52 by utilizing dispersion consisting of plates chemically modified with 1-chloroethyltrichlorosilane and a mixture of 1,4-dichlorobutane and *n*-hexane. The deposition probabilities of the plates primarily depended on the type of solvent for plate dispersions and increased with an increase in the value of free energy change of the plate/solvent/water system by the movement of the plate from the solvent to the solvent/water interface during the blade-coating process. These results indicate that the deposition probabilities are governed directly by the capillary force acting on the plates. Our deposition technique for microstructures using blade-coating is potentially applicable to the deposition of micrometer-size electronic devices on large-scale substrates.

I. Introduction

Robotic serial assembly techniques are used for integrating various types of electronic devices on substrates to fabricate functional electronic appliances, such as motherboards, flat panel displays, and mobile phones. Although these techniques have contributed to key technologies for the fabrication of electronic appliances, they are encountering difficulties in assembling devices with sizes smaller than several hundred micrometers: they risk being damaged by robotic hands, and loading speed slows with decreasing device size, resulting in higher loading costs.[1,2]

Various strategies have been proposed for loading micrometer-size devices onto substrates, which include wafer-to-wafer transfer and fluidic self-assembly methods.[3−23] Fluidic self-assembly (FSA) methods hold promise for realizing the assembly of large numbers of microstructures on substrates, since these processes can simultaneously deposit large numbers of microstructures on specific areas of substrates at high yields, resulting in a very high assembly speed. In a typical process of FSA, a large number of freestanding microstructures are fabricated separately and then dispersed in a carrier fluid. The binding sites for the microstructures are fabricated on the surface of the substrate. After placing the substrate in a suitable liquid, the dispersion of microstructures is injected into the liquid such that the microstructures flow over the substrate. In this process, the microstructures come close to the binding sites and are pulled there spontaneously by gravity, electrostatic force, magnetic force, or capillary force.

Our final target is to develop a fluid self-assembly method suitable for the mass production of electronic appliances. Our strategy for achieving this is to develop a printing method that utilizes the FSA mechanism, since printing methods are widely used for large-scale electronic appliances at low cost, such as liquid crystal displays, plasma displays and solar cells, and thus should be suitable for mass production.

On the other hand, we have already presented a novel blade-coating technique that takes advantage of capillary force for rod-shaped silicon nanowires (NWs) of nanometer to micrometer-size on selected areas of substrates.[24] Our blade-coating technique consists of a continuous blade-coating process using water followed by NW dispersions onto the substrate on which surface hydrophilic areas are surrounded by a hydrophobic self-assembled monolayer. The NW dispersion consists of NWs chemically modified with 1-chloroethyltrichlorosilane and 1,4-dichlorobutane, which have low solubility in water. In this process, first, water is selectively placed on the hydrophilic areas; second, the NW dispersion covers the water to create a dispersion/water interface; and third, the NWs are pulled into the interface by capillary force. Finally, the NWs are deposited onto the hydrophilic areas after the evaporation of the water and the solvent of the dispersion. Using this method, NWs were selectively deposited on hydrophilic areas of substrates with a probability of 0.99. We believe that if this technique is applicable to the deposition of micrometer-sized devices on substrates, it can be developed into a mass production method for fabricating electronic appliances. In previous experiments, we tried to deposit micrometer-size plates sized 10×50 μm^2 and with a thickness of 0.3 μm, which were models of switching transistors

* To whom corresponding should be addressed. E-mail: arase.hidekazu@jp.panasonic.com.

10.1021/jp9070289 CCC: $40.75
Published on Web 10/27/2009

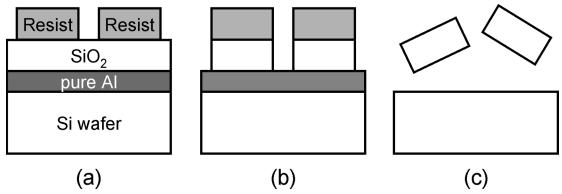

Figure 1. The process of SiO_2 plate fabrication. (a) A photomicrographic process is applied to the wafer to make posi-resist patterns, (b) the top of SiO_2 layer is dry-etched, and (c) the Al sacrificial layer is selectively etched, after which the SiO_2 plates separate from the wafer.

for individual pixels in an electroluminescence display, on hydrophilic areas of $10 \times 50\ \mu m^2$. However, the deposition probability of the plates was a very low 0.1, much smaller than that for NWs.

The purpose of this paper is to improve our blade-coating technique such that it enables the depositing of micrometer-size plates on selected areas with a high deposition probability comparable to that of NWs. In this paper, we redesigned the plate dispersion to accomplish this purpose. It appears that the deposition probabilities of the plates depend primarily on the type of solvent used for the plate dispersion. Using an optimized solvent, the SiO_2 plates were deposited on selective areas with a deposition probability of over 0.5. We discuss the mechanism that governs the deposition probability from the viewpoint of the free energy of the plate/solvent/water system during the blade-coating process.

II. Experimental Section

A. Preparation of Dispersions of SiO_2 Plates. We used ($10 \times 50 \times 0.3$) μm rectangular SiO_2 plates for the deposition experiments instead of using actual electronic devices. The size of the SiO_2 plates corresponds to that of switching transistors for 50-in. and larger electroluminescence displays, one of our targets. Since the surface energy of the microstructure surface plays a key role in depositing the microstructures on substrates, it is desirable to choose a material for the microstructures that can be readily chemically modified to change its surface energy (see the blade-coating method). Thus, we used SiO_2, whose surface has silanol groups that react with silane coupling agents. We used these chemically modified SiO_2 plates to deduce the basic principles of deposition of the microstructures applied using our method.

Figure 1 shows the process for fabricating SiO_2 plates. An Al sacrificial layer 200 nm thick and a SiO_2 layer 0.3 μm thick were deposited on a silicon wafer by sputtering and plasma-enhanced chemical vapor deposition, respectively. A photolithographic process was then applied to the wafer to make posi-resist patterns in the form of rectangles whose longitudinal side lengths were 50 μm and horizontal side lengths were 10 μm, as shown in Figure 1a. The SiO_2 layer not covered with photoresist was dry-etched, as shown in Figure 1b. The silicon wafer was then immersed in a $H_3PO_4/HNO_3/CH_3COOH$ solution (4:1:1 in volume) at 50 °C for 15 min. In this process, the Al sacrificial layer was selectively etched, and the SiO_2 plates left the wafer to disperse into the solution, as shown in Figure 1c. The solution containing SiO_2 plates was filtered via a polytetrafluoroethylene (PTFE) membrane filter to separate the SiO_2 plates from the solution. After filtering the dispersion, the SiO_2 plates were adsorbed onto the surface of a PTFE membrane filter. This PTFE membrane filter with adsorbed SiO_2 plates was then carefully rinsed with deionized water (twice), acetone (twice), and dehydrated methanol (twice). It was then immersed in 1 vol % 1-chloroethyltrichlorosilane in 1,4-dichlorobutane solution for 2 h, followed by rinsing with 1,4-dichlorobutane several times in a dry nitrogen atmosphere. In this process, the surfaces of the SiO_2 plates are chemically modified by 1-chloroethyltrichlorosilane. Finally, the chemically modified SiO_2 plates were separated from the PTFE membrane and dispersed into various water-insoluble organic solvents 20 mL in volume—*n*-hexane, 1,4-dichlorobutane, mixtures of *n*-hexane and 1,4-dichlorobutane, mixtures of *n*-decane and 1,4-dichlorobutane, and mixtures of cyclohexane and 1,4-dichlorobutane—by gently agitating the PTFE membrane filter in these solvents. The concentrations of SiO_2 plates in the dispersions were estimated to be 2.0×10^6/mL by rough calculation from the volume of the dispersions and the number of Si wafers used for preparing the SiO_2 plate dispersions.

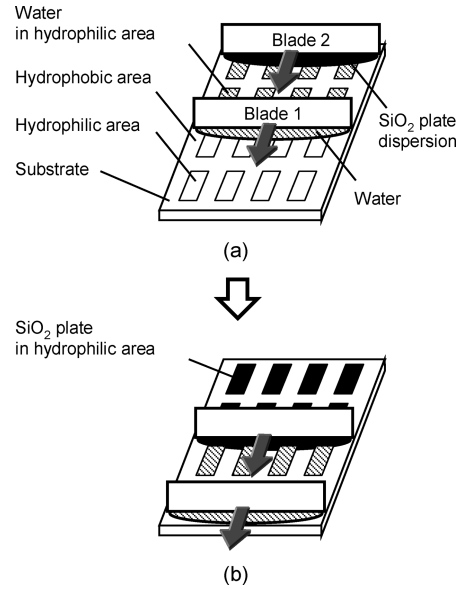

Figure 2. Schematic images of the SiO_2 plate deposition method, comprising two steps: (a) first, water is coated by blade 1 onto the chemically patterned substrate surface where hydrophilic areas are surrounded by a hydrophobic self-assembled monolayer, selectively depositing water on the hydrophilic areas; (b) second, before the evaporation of the water, the SiO_2 plate dispersion is coated by blade 2 onto the same surface. In this step, the dispersion comes into contact with the water.

B. Preparation of Chemically Modified Substrates. A 4-in.-diameter silicon wafer, covered with silicon nitride, was cleaned by oxygen plasma. A photomicrographic process was applied to the wafer to make resist patterns in the form of rectangles whose longitudinal side lengths were 50 μm and horizontal side lengths were 10 μm, lined up in a lattice pattern with an average spacing of 100 μm. The wafer was immersed in 1 vol % 2-perfluorooctylethyltrichlorosilane (FAS) solution in perfluorobutyl ethyl ether for 2 h, followed by rinsing with perfluorobutyl ethyl ether several times in a dry nitrogen atmosphere. The resist films were removed from the wafer by dipping it in acetone. During these procedures, FAS adsorbs onto only surfaces that are not covered with the resist films. Because the silicon nitride surface is hydrophilic and the self-assembled monolayer from FAS is hydrophobic, the hydrophilic rectangle areas were surrounded by a hydrophobic area on the wafer.

C. Blade-Coating Deposition Experiment. The deposition method of SiO_2 plates on the chemically modified substrate is the same as that reported previously[24] and is shown briefly, as follows. Figure 2 shows the principle of our method in schematic form. First, water is blade-coated onto the chemically patterned

substrate, on which hydrophilic areas are surrounded by a hydrophobic self-assembled monolayer. In this step, water is selectively placed on the hydrophilic areas, as shown in Figure 2a. Second, before the water evaporates, the SiO_2 plate dispersion is blade-coated onto the same surface. The dispersion comes into contact with the water, as shown in Figure 2b. We chose a water-insoluble solvent for dispersing SiO_2 plates and chemically modified plates by 1-chloroethyltrichlorosilane such that they tend to be adsorbed onto the solvent/water interface by capillary force. After blade-coating of the SiO_2 plate dispersion, the SiO_2 plates remain at the solvent/water interface. The SiO_2 plates adsorb onto the hydrophilic areas during the evaporation of the water and the solvent.

We used a homemade blade-coater with one stainless steel plate (blade 1) for coating water and one glass plate (blade 2) for coating the SiO_2 plate dispersions. Both plates measured 50 mm long by 30 mm wide by 1 mm thick. Each blade was set with its surface facing a 2-mm spacing, and their edges faced the substrate at a distance of 0.2 mm. Water and SiO_2 dispersion were injected via glass pipettes between the plate edges and the surface of substrate to allow the meniscus to create a liquid curtain. Both plates were moved simultaneously at a velocity of 10 mm/s parallel to the longitudinal sides of the hydrophilic rectangular areas on the surface so that first the water and then the plate dispersion were coated on the surface.

D. Calculation of Interfacial Tension. The interfacial tensions between the SiO_2 plate and the water, $\gamma_{p/W}$; between the SiO_2 plate and solvent of the plate dispersion, $\gamma_{p/d}$; and between the water and the solvent of the plate dispersion, $\gamma_{W/d}$, were obtained experimentally to examine the relationship between the deposition probability and the free energy change of a plate/solvent/water system during blade-coating the water and the plate dispersion. We assumed that the surface free energy of the chemically modified SiO_2 plate, γ_p, is the same as that of the silicon substrate covered with thin SiO_2 film, γ_S, which was chemically modified using the same method as that for the SiO_2 plate, and thus, $\gamma_{p/W}$ and $\gamma_{p/d}$ are the same as the interfacial tension between the chemically modified silicon substrate and water, $\gamma_{S/W}$, and between the chemically modified substrate and organic solvent, $\gamma_{S/d}$, respectively. Since the $\gamma_{S/W}$ and $\gamma_{S/d}$ can be calculated from the γ_S and static contact angles of the organic solvents on the chemically modified silicon substrate, we first calculated the surface free energy components of the chemically modified silicon substrate using Van Oss−Chaudhury−Good eqs 1 and 2,[25,26]

$$\gamma_L(1 + \cos\theta) = 2\left(\gamma_S^{LW}\gamma_L^{LW}\right)^{1/2} + 2\left(\gamma_S^{+}\gamma_L^{-}\right)^{1/2} + 2\left(\gamma_S^{-}\gamma_L^{+}\right)^{1/2} \quad (1)$$

$$\gamma_S = \gamma_S^{LW} + 2\left(\gamma_S^{+}\gamma_S^{-}\right)^{1/2} \quad (2)$$

where γ_i is the surface tension, the subscripts S and L represent the chemically modified substrate and liquid, respectively, the superscripts LW, +, and − refer to the apolar (Lifsitz−van der Waals) component, the electron acceptor (Lewis acid) component, and the electron donor (Lewis base) component, respectively; and θ is the static contact angle of the liquid on the substrate. The value of γ_S was obtained as 43.3 mJ/m^2 by measuring the contact angles of three different liquids: water, ethylene glycol, and diiodomethane, whose γ_L, γ_L^{LW}, γ_L^{+}, and γ_L^{-} values are known.[27]

The values of $\gamma_{S/W}$ and $\gamma_{S/d}$ are calculated from eqs 3 and 4, respectively,

$$\gamma_s = \gamma_W \cos\theta_W + \gamma_{s/W} \quad (3)$$

$$\gamma_s = \gamma_d \cos\theta_d + \gamma_{s/d} \quad (4)$$

where γ_W, γ_d, θ_W, and θ_d are the surface tension of water and solvent and the static contact angle of water and solvent, respectively, on the chemically modified silicon substrate. The γ_W and γ_d values were measured using the ring method. The $\gamma_{W/d}$ value was measured using the pendant drop method. The values of $\gamma_{W/d}$ and $\gamma_{S/d}$ are summarized in Table 1. Table 1 also includes the values of the interfacial tensions, $\gamma_{S/W}$.

III. Results and Discussion

Figure 3 shows dark-field optical micrographic images of the substrates (a) after 5 blade-coating cycles of dispersion A, (b) after 5 blade-coating cycles of dispersion E, and (c) after 10 blade-coating cycles of dispersion E. The number of plates on the substrates after blade-coating dispersion E was much greater than that after dispersion A, as shown in Figure 3, indicating that the deposition probability depends on the type of solvent for the plate dispersions. The number of SiO_2 plates on the substrate tends to increase on increasing the blade-coating cycles, as shown in Figure 3b and c, as will be discussed later. After blade-coating dispersion E, most plates on the substrates were aligned parallel to the direction of blade-coating and lined up in the lattice pattern with an average spacing of 100 μm. Since the configuration of the SiO_2 plates was the same as that of the hydrophilic areas, the SiO_2 plates should be selectively positioned on the hydrophilic areas. The deposition states of SiO_2 plates could be classified into three groups: group I, SiO_2 plates are correctly deposited in the hydrophilic area and thus aligned parallel to the longitudinal direction of the area; group II, SiO_2 plates are not completely deposited in the hydrophilic area and inclined in the longitudinal direction of the hydrophilic area; and group III, multiple SiO_2 plates are located in a hydrophilic area and adhere to each other. The origin of the deposition failure of group II is likely to be caused by the decrease in water volume in the hydrophilic area during the blade-coating process. In our method, just after the water is blade-coated on the hydrophilic areas on the substrate, the plate dispersion is blade-coated on the same areas, such that the SiO_2 plate comes into contact with the water deposited on the hydrophilic areas. After contact of the plate with water, the plates are pulled into the hydrophilic areas by capillary force. However, some of the water settles in only part of the hydrophilic area because "hydrophobic" contaminations in the hydrophilic area, generated by experimental circumstances, prevent the water from coating the entire hydrophilic area during water blade-coating. In this case, the plates cannot be deposited correctly in the hydrophilic area and are located out of the area. Plates in group III predominate on the substrate with increasing blade-coating cycles. We speculate that the plates are deposited step-by-step by repeated blade-coating. After the deposition of the plate in a hydrophilic area, the next blade-coating process is performed. In this process, water is selectively deposited not only on hydrophilic areas where plates are absent, but also on the hydrophilic areas where the plates were deposited in the previous blade-coating process. Water deposition on the SiO_2 plates should occur because the chemically modified SiO_2 surface is more hydrophilic than that of the hydrophobic FAS monolayer area: the static contact angle of water on the chemically modified SiO_2, 60°, is smaller than that of FAS monolayer, 108°. By blade-coating the SiO_2 plate dispersion, the plates adsorb onto

TABLE 1: Molar Ratios of the Solvents for Plate Dispersions and Interfacial Tensions, $\gamma_{W/d}$, $\gamma_{S/d}$, and $\gamma_{S/W}$

	dispersion liquid		molar ratio		interfacial tension (mJ/m^2)		
dispersion	solvent 1	solvent 2	solvent 1	solvent 2	$\gamma_{W/d}$	$\gamma_{S/d}$	$\gamma_{S/W}$
A	1,4-dichlorobutane		1.00	0	31.8	5.4	7.1
B	1,4-dichlorobutane	*n*-decane	0.84	0.16	31.9	13.5	7.1
C	1,4-dichlorobutane	*n*-hexane	0.78	0.22	32.3	11.8	7.1
D	1,4-dichlorobutane	*n*-decane	0.64	0.36	34.8	16.3	7.1
E	1,4-dichlorobutane	*n*-hexane	0.54	0.46	36.4	18.0	7.1
F	1,4-dichlorobutane	cyclohexane	0.52	0.48	33.9	15.3	7.1
G		*n*-hexane	0	1.00	47.0	22.2	7.1

plates previously deposited on the hydrophilic area, resulting in multiple plate deposition.

Figure 4 shows the deposition probability dependence on the blade-coating cycles with dispersions A (closed triangles) and E (closed circles). The deposition probability was deduced as follows using an optical microscope: After blade-coating, 1000 hydrophilic areas, randomly selected from the substrates, were observed by microscopy. The deposition probability was deduced by dividing the total number of hydrophilic areas in which SiO_2 plates were correctly deposited (group I) by the number of hydrophilic areas observed. The probability with Ddispersion A was 0.02 for the first cycle, 0.04 for the third cycle and 0.06 for the fifth cycle. The probability with dispersion A saturated at around 0.1 over 5 cycles. In contrast, the probability with dispersion E was much greater than that with dispersion A: 0.17 for the first cycle and 0.38 for the third cycle; it increased with more cycles to reach 0.52 for the fifth cycle. The SiO_2 plates appear to be progressively deposited on empty hydrophilic areas by repeating blade-coating, resulting in an increase in the deposition probability with the blade-coating cycles. However, with more cycles, the deposition probability dropped to 0.17 for the 10th cycle. The drop of the probability at the 10th cycle is caused from an increase in the number of the plates in group III by repeating blade-coating. Although 97% of hydrophilic areas are filled with SiO_2 plates at the 10th cycle, 80% of the SiO_2 plates on the hydrophilic areas are classified into group III, resulting in low probability. Detailed observations of the SiO_2 plates in group III showed that almost all the plates contacting with substrate are correctly deposited in hydrophilic areas, and the other plates adsorb onto them. By establishing the method for avoiding multiple depositions of the plates, the deposition probability achieves at least 0.97, and our technique can be applied to fabricate electronic appliances.

The probability dependence on blade-coating cycles with various solvents is summarized in Table 2. The deposition probability with dispersion E was the greatest in those with the other dispersions. With dispersion E, we deposited about 40 000 SiO_2 plates on the hydrophilic areas on the substrate with a 20

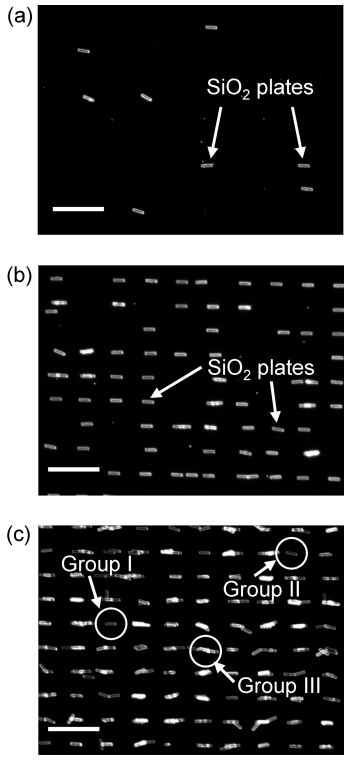

Figure 3. Optical dark-field microscopy images of the chemically patterned substrates (a) after 5 blade-coating cycles of dispersion A, (b) after 5 blade-coating cycles of dispersion E, and (c) after 10 cycles of dispersion E. The hydrophilic 10 × 50 μm^2 areas on the substrate lined up in the lattice pattern with an average spacing of 100 μm. The white areas correspond to SiO_2 plates. The white line bar at the lower left of the image represents 200 μm. In this image, the blade-coating direction of the SiO_2 dispersion corresponds to the horizontal direction.

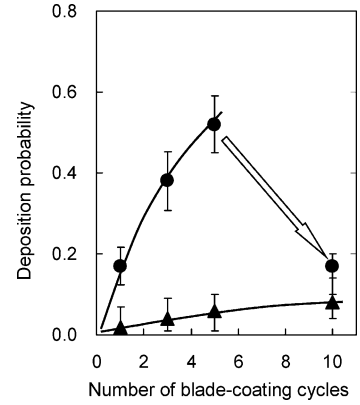

Figure 4. Dependence of the deposition probability of SiO_2 plates onto 10 × 50 μm^2 hydrophilic areas on blade-coating cycle with dispersions A (closed triangles) and E (closed circle). The probability was estimated from 1000 hydrophilic areas on a substrate.

TABLE 2: Free Energy Change *E* and Deposition Probabilities for the 5th Cycle

	free energy difference, *E* (10^{-12} J)		
dispersion	*E1*	*E2*	deposition probability (fifth cycle)
A	−15.1	1.7	0.06
B	−19.1	−6.4	0.20
C	−18.5	−4.7	0.19
D	−22.0	−9.2	0.43
E	−23.6	−10.9	0.52
F	−21.1	−8.2	0.34
G	−31.0	−15.1	NA[a]

[a] The SiO_2 plates aggregated in n-hexane.

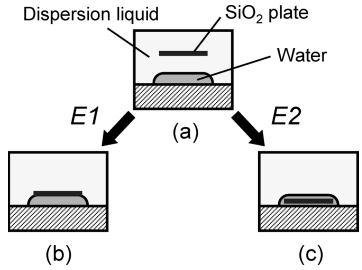

Figure 5. Schematic sectional images of the three states around the interface. (a) SiO_2 plates dispersed in the solvent, (b) SiO_2 plates adsorbed onto the solvent/water interface, and (c) the SiO_2 plates completely immersed in the water.

cm^2 area with a probability of 0.52. Because one cycle of the coating is complete within 30 s in our method, it takes only 3 min. These results demonstrate that our method is suitable for depositing a large number of microstructures and is potentially applicable to the deposition of micrometer-size electronic devices for fabricating electronic appliances.

The deposition probability of the SiO_2 plates achieves 0.52 for the fifth cycle of blade-coating with dispersion E, which is the most suitable dispersion for depositing the plates efficiently. On the other hand, we previously reported that the deposition probability of rod-shaped NWs achieves 0.99 for the fourth cycle of blade-coating with the same solvent as dispersion A,[24] which is not suitable for depositing plates with high probability, as shown in Table 2. These results indicate that the deposition efficiency of plates is much smaller than that of NWs. The deposition difference between SiO_2 plates and the NWs appears to be due to the difference in the ratio of the size of the hydrophilic area to the size of one NW or one SiO_2 plate. SiO_2 plates sized $10 \times 50\ \mu m^2$ were deposited on hydrophilic areas sized $10 \times 50\ \mu m^2$ (giving a ratio of 1); on the other hand, NWs sized about $15 \times 0.1\ \mu m^2$ were deposited on hydrophilic areas measuring $2 \times 15\ \mu m^2$ (the ratio is 20). In our previous work, the deposition probability increased with an increased ratio.[24] It is reasonable that the deposition efficiency of plates with a ratio of 1 is much smaller than that of NWs with a ratio of 20.

In our previous work, we confirmed, from the free energy calculation of the NW/solvent/water system, that NWs are adsorbed on the solvent/water interface.[24] Although the size of the SiO_2 plates used in this work is greater than that of a NW, it is also difficult to observe the adsorption process directly, since it occurs on a micrometer scale and within 1 s. Thus, we estimated the adsorption process of the plates in the hydrophilic area on the basis of a free energy calculation similar to that for NWs.

Figure 5 shows schematic sectional images of three states of the plate/solvent/water system. In this system, each SiO_2 plate (a) disperses in the solvent, (b) adsorbs on the solvent/water interface, or (c) is completely immersed in the water. The values of the free energy change between states a and b, E1, and the free energy change between states a and c, E2, are deduced from eqs 5 and 6, respectively,

$$E1 = -S(\gamma_{W/d} + \gamma_{S/d} - \gamma_{S/W}) \quad (5)$$

$$E2 = -2(S + s)(\gamma_{S/d} - \gamma_{S/W}) \quad (6)$$

where S and s indicate the area of the plate face ($10 \times 50\ \mu m^2$) and edge ($0.3 \times 60\ \mu m^2$), respectively. The calculated values

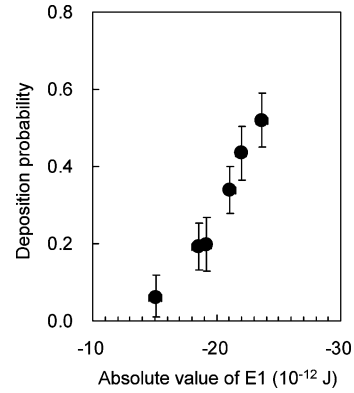

Figure 6. Dependence on the absolute value of free energy change E1 of the deposition probability of SiO_2 plates onto $10 \times 50\ \mu m^2$ hydrophilic areas.

of E1 and E2 are summarized in Table 2. All the values of E1 and E2 are negative. The value of E1 was smaller than that of E2 in each of the dispersions. These results indicate that the SiO_2 plate adsorbed onto the solvent/water interface instead of immersing into the water so as to minimize the free energy of the system during the blade-coating process. The capillary force acts on the SiO_2 plate to pull into the solvent/water interface and minimizes the free energy. After the blade-coating of water and SiO_2 plate dispersion, the water and the SiO_2 plate dispersion remain in the hydrophilic areas, where SiO_2 plates adsorb onto the solvent/water interface. The SiO_2 plates migrate to the hydrophilic areas during the evaporation of the water and the solvent.

Figure 6 shows the deposition probability dependence on the absolute value of E1 (|E1|). The deposition probability increased with an increase of the value of |E1|. We speculate that the dynamic process of the plate movement contributes to the probability. The adsorption process of the plate on the solvent/water interface starts at the first step, where only a part of the plate contacts the interface. Since the plates in the dispersion align their long sides parallel to the direction of the blade-coating due to the dispersion flow, the short side of the plate comes into contact with the interface, and thus, the contact area is very small at the first step. All the values of |E1| are calculated from eq 5 on the condition that the whole area of the plate face ($10 \times 50\ \mu m^2$) contacts the interface and about 5 orders of magnitude greater than the kinetic and potential energies that disturb the movement of the plate on the solvent/water interface.[28] On the other hand, at the first step, the contact area is very small, and the free energy change, defined by e1 (the absolute value of e1 is |e1|), due to the contact of only a part of the plate with the interface should be small and compatible that of the kinetic energy or potential energy. The deposition probabilities are governed by the first step, where the energy balances among kinetic energy, potential energy, and |e1| determine the probability, and thus, they increase with an increase in |e1|. The values of |e1| could be deduced from eq 5 by changing only the contact area, S, without changing other parameters, indicating that the order of |e1| values of various types of solvents for plate dispersions should be the same as that of |E1|, and thus, the deposition probability increased with an increase in the value of |E1|, as shown in Figure 6.

It is also important to consider the volume of the water deposited on hydrophilic areas for clarification of the deposition mechanism. The small water drops on the hydrophilic areas will evaporate rapidly and also may be dissolved very slightly in the solvent. As a result, its volume will decrease. This decrease

in the volume of the water might also affect the deposition probability. However, both the detailed dynamic process of the plate deposition and the volume change of the water in the hydrophilic area remain unclear. It will be necessary to observe directly the dynamic process of plate movement and the volume change of the water in the solvent using a high-speed microscope camera to elucidate the deposition mechanism of the microstructures on the substrate, which will be reported elsewhere.

IV. Conclusions

A novel blade-coating technique for the fluidic self-assembly of microstructures onto selected areas on large-scale substrates is presented. This technique will be applicable to deposition of micrometer-size electronic devices. Using this technique, about 40 000 SiO_2 plates sized $10 \times 50 \times 0.3$ μm^3 were selectively deposited on the hydrophilic areas of a substrate with an area of 20 cm^2 with a deposition probability of 0.52 by utilizing plate dispersion with plates chemically modified with 1-chloroethyltrichlorosilane and a mixture of 1,4-dichlorobutane and hexane. We found that the deposition probabilities of the plates depended to a great extent on the type of the solvent used for the plate dispersions and that the deposition probability was governed by the free energy change, |E1|.

Our technique has potential for application to the manufacture of large-scale electronic appliances and for scaling up for mass production. We have not yet established the ultimate deposition techniques in terms of high deposition probability and alignment accuracy. It is necessary to achieve a high deposition probability with minimum blade-coating cycles and accurate deposition on the hydrophilic areas to enhance the potential of our method for mass production. To accomplish this, it is important to choose the appropriate solvents to maximize the |E1| of the plate/solvent/water system to achieve high deposition probability. It is also important to clarify the relationship between the plate alignment and the volume of water, both in hydrophilic areas and on plates previously deposited on hydrophilic areas to develop the method for achieving accurate deposition. These studies are in progress at our laboratory.

Acknowledgment. We thank Dr. Daisuke Ueda and Dr. Eiji Fujii for fruitful discussions and are also grateful to Mr. Akihiro Itoh for his experimental support and advice.

References and Notes

(1) Morris, C. J.; Stauth, S. A.; Parviz, B. A. *IEEE Trans. Adv. Packag.* **2005**, *28*, 600.

(2) Cohn, M. B.; Böhringer, K. F.; Noworolski, J. M.; Singh, A.; Keller, C. G.; Goldberg, K. Y.; Howe, R. T. Microassembly Technologies for MEMS. *Proceedings of SPIE Micromachining and Microfabrication, Conference on Micromachining and Microfabrication Process Technology IV*, Santa Clara, CA, Sept 21−22, 1998; pp 2−16.

(3) Stauth, S. A.; Parviz, B. A. *Proc. Natl. Acad. Sci., U.S.A.* **2006**, *103*, 13922.

(4) Lee, K. J.; Lee, J; Hwang, H; Reitmeier, Z. J; Davis, R. F; Rogers, J. A.; Nuzzo, R. G. *Small* **2005**, *1*, 1164.

(5) Lee, K. J.; Meitl, M. A.; Ahn, J.; Rogers, J. A.; Nuzzo, R. G.; Kumar, V.; Adesida, I. *J. Appl. Phys.* **2006**, *100*, 124507.

(6) Yeh, H.-J. J.; Smith, J. S. *IEEE Photonics Technol. Lett.* **1994**, *6*, 705.

(7) Terfort, A.; Bowden, N.; Whitesides, G. M. *Nature* **1997**, *386*, 162.

(8) Tien, J.; Breen, T. L.; Whitesides, G. M. *J. Am. Chem. Soc.* **1998**, *120*, 12670.

(9) Breen, T. L.; Tien, J.; Oliver, S. R. J.; Hadzic, T.; Whitesides, G. M. *Science* **1999**, *284*, 948.

(10) Jacobs, H. O.; Tao, A, R.; Schwartz, A.; Gracias, D. H.; Whitesides, G. M. *Science* **2002**, *296*, 323.

(11) Terfort, A.; Whitesides, G. M. *Adv. Mater.* **1998**, *10*, 470.

(12) Bowden, N.; Oliver, S. R. J.; Whitesides, G. M. *J. Phys. Chem. B* **2000**, *104*, 2714.

(13) Syms, R. R. A.; Yeatman, E. M.; Bright, V. M.; Whitesides, G. M. *J. Microelectromech. Syst.* **2003**, *12*, 287.

(14) Srinivasan, U.; Liepmann, D.; Howe, R. T. *J. Microelectromech. Syst.* **2001**, *10*, 17.

(15) Xiong, X.; Hanein, Y.; Fang, J.; Wang, Y.; Wang, W.; Schwarz, D. T.; Böhringer, K. F. *J. Microelectromech. Syst.* **2003**, *12*, 117.

(16) Schott, K. L.; Hirano, T.; Yang, H.; Singh, H.; Howe, R. T.; Niknejad, A. M. *J. Microelectromech. Syst.* **2004**, *13*, 300.

(17) Onoe, H.; Matsumoto, K.; Shimoyama, I. *J. Microelectromech. Syst.* **2004**, *13*, 603.

(18) Murakami, Y.; Idegami, K.; Nagai, H.; Yamamura, A.; Yokoyama, K.; Tamiya, E. *Proceedings of IEEE Workshop on Micro Electro Mechanical Systems (MEMS)*, Switzerland, 2001, pp 369−374.

(19) Nakakubo, T.; Shimoyama, I. *Sens. Actuators* **2000**, *A83*, 161.

(20) Soga, I.; Ohno, Y.; Kishimoto, S.; Maezawa, K.; Mizutani, T. *Jpn. J. Appl. Phys.* **2003**, *42*, 2226.

(21) Zheng, W.; Jacobs, H. O. *Adv. Mater.* **2006**, *18*, 1387.

(22) Zheng, W.; Buhlman, P.; Jacobs, H. O. *Proc. Natl. Acad. Sci. U.S.A.* **2004**, *101*, 12814.

(23) Sharma, R. *Langmuir* **2007**, *23*, 6843.

(24) Nakagawa, T.; Torii, H.; Kawashima, T.; Saitoh, T. *J. Phys. Chem. C* **2008**, *112*, 5390.

(25) Van Oss, C. J.; Chaudhury, M. K.; Good, R. J. *Chem. Rev.* **1988**, *88*, 927.

(26) Van Oss, C. J.; Good, R. J.; Chaudhury, M. K. *Langmuir* **1988**, *4*, 884.

(27) Good, R. J. Contact angle, wetting, and adhesion: A critical review. In *Contact Angle, Wettability and Adhesion*; Mittal, K. L., Ed.; 1993; vol. *VSP BV*; pp 3−36.

(28) The kinetic energy of the SiO_2 plate is calculated to be roughly 1.7×10^{-5} pJ using the mass of a SiO_2 plate and the blade-coating velocity of 10 mm/s. The potential energy of the SiO_2 plate in dispersion E is calculated to be roughly 3.8×10^{-4} pJ by multiplying the weight of a SiO_2 plate in the dispersion by a height 0.2 mm, which is a distance between the substrate and the blade edge faced the substrate.

JP9070289